Biophysical Journal, Volume *112*

Supplemental Information

Design and Properties of Genetically Encoded Probes for Sensing Macromolecular Crowding

Boqun Liu, Christoffer Åberg, Floris J. van Eerden, Siewert J. Marrink, Bert Poolman, and Arnold J. Boersma

Materials. Chemicals were obtained from Sigma-Aldrich at the highest available purity, and used without further purification, unless noted otherwise.

Fluorescence recovery after photobleaching (FRAP)

Cells were grown as for the FRET measurements in confocal microscopy. The cells were harvested by centrifugation and washed by MOPS minimal medium without glucose and potassium phosphate. The cells were subsequently resuspended with desired concentration NaCl in MOPS minimal medium without glucose and potassium phosphate and immediately placed on a coverslip. Both photobleaching and excitation were carried out using a 480 nm laser (with different intensities). The emission was collected from 493 nm to 797 nm. We focused on a cell using low laser intensity, and an area at one side of the bacterium was bleached using a diffraction-limited laser beam of high intensity. Immediately after that a series of images was collected using the low intensity laser beam to capture the fluorescence recovery process. The resolution of the images was 16×16 pixels. The diffusion coefficients were calculated as reported previously.[1,2]

Modeling effect of linker length and flexibility on FRET efficiency in the absence of crowding

Because of the linker being rather flexible and because we are interested in qualitative features, we may approximate the Gn family as simple ideal chains.[3,4] Assuming an ideal chain, the probability, $P(r)\mathrm{d}r$, of a given end-to-end distance, r, is given by

$$P(r)\mathrm{d}r = \left(\frac{3}{2\pi Ll}\right)^{3/2} \exp\left(-\tfrac{3}{2}r^2/(Ll)\right) 4\pi r^2 \mathrm{d}r \qquad \text{(S2)}$$

where L is the extended length of the linker and l is the length of a Kuhn segment.

The FRET efficiency can then be evaluated as the average

$$\left\langle \frac{1}{1+(r/R_0)^6} \right\rangle = \int \frac{P(r)\mathrm{d}r}{1+(r/R_0)^6} \qquad \text{(S3)}$$

where R_0 is the Förster radius. With a Förster radius of R_0 = 5.4 nm and a Kuhn length of l = 2 nm this results in the relation between FRET efficiency and linker length shown in Figure 1C (black).

For the EmGn families we approximate the linker by an ideal chain and two completely rigid rods, randomly oriented, in succession. The probability, $P(r)\mathrm{d}r$, of a given end-to-end distance is readily found by stochastic numerical simulation: choosing a length of the ideal chain part from the distribution in Eq. S2 and choosing the orientations of the two rigid rods uniformly over the surface of the sphere, followed by calculating the FRET efficiency from the first equality of Eq. S3. Using a rigid rod length of 3.01 nm (E4Gn) and 4.35 nm (E6Gn), respectively, results in the relation shown in Figure 1C (red and blue, respectively).

Using these simple models it may be observed how, for a given length of the linker, replacement of part of a flexible linker with a completely rigid part lowers the observed FRET efficiency (Figure 1C arrow). Furthermore, the FRET efficiency is lowered more the longer the rigid part of the linker. All in all, the same qualitative observations as made experimentally (Table 1). More sophisticated models (potentially also including the fluorescent proteins) will

give different parameters and may yield better quantitative agreement. However, most likely this would not change the qualitative picture.

Table S1. Composition of simulated systems. Type of sensor and crowding agent, number of CG water beads (note, the corresponding number of real water molecules is four times bigger), amount of PEG136 polymer chains, number of ubiquitin proteins, and number of Na^+ and Cl^- ions, respectively.

System	Water	PEG	UBQ	Na^+	Cl^-
GE	205617	0	0	2334	2317
GE UBIQ	174913	0	311	1986	1969
GE PEG	145588	441	0	1826	1809
G18	90943	0	0	1037	1020
G18 UBIQ	75205	0	161	859	842
G18 PEG	64401	189	0	817	800

Table S2: Comparison of the actual distance between fluorophores, and the apparent distance calculated from the FRET efficiencies using the Förster equation. Both distances were determined from molecular dynamics simulations as described above.

	GE		G18	
	Distance from MD (nm)	Distance from FRET[a] (nm)	Distance from MD (nm)	Distance from FRET[a] (nm)
No crowder	12.1±0.2	9.8±0.2	8.1±0.05	7.3±0.04
Ubiquitin	11.4±0.7	9.1±0.5	7.6±0.4	6.9±0.2
PEG 6 kD	6.4±0.6	5.9±0.2	4.9±0.8	5.2±0.9

[a] Calculated with the Förster equation from the FRET efficiencies, which in turn are determined by the molecular dynamics simulations as described in the materials and methods section. To understand the reason behind the difference between these distances we note that the distance from FRET is from a large set of conformations. Within the population of conformations, the smaller distances contribute more to this average FRET due to the dependence of the FRET efficiency on the distance. Hence calculating the distance from FRET from a population of conformations will give a separation that is different from the average distance. Because the efficiencies are rather low, the direction of the deviation is mostly the same. This reasoning also applies to our "wet" experiments where there are always a large number of conformations

sampled at a given time interval. If we were to correct for this deviation, it would require knowledge of the distribution of states that the sensor populates. In molecular dynamics simulations we can measure all states in one molecule individually; this allowed us to compare the "real" radius with an "ensemble" FRET.

Table S3. Detailed characteristics of the linkers.

Acronym	Amino acids in linker	Extended linker length (nm)[a]	Measured distance from FRET (nm)	EAAAK/GSG ratio
GE	114	34.71	7.6±0.2	0.67
E6G6	78	22.13	7.3±0.1	2
E6G2	66	17.97	7.3±0.1	6
E4G6	58	19.45	6.7±0.1	1.3
E4G2	46	15.29	6.6±0.1	4
E6	66	23.92	6.6±0.1	0.5
G24	72	32.0	6.3±0.1	0
G18	54	25.71	6.0±0.1	0
G12	36	19.42	5.7±0.1	0

[a] Extended linker length was determined by model building in Pymol, with α-helical backbone conformations for the helical regions and parallel β-sheet for the random coil domains. The C- to N-terminus distance was measured with the distance measuring tool in Pymol.

Table S4: Partial specific volumes used to calculate crowder volume fractions. Especially for Ficolls and dextrans various values, generally between 0.61 and 0.67 mL/g, have been reported in the literature. Despite these different values (that are often within the measurement error of the reported methods), the differences are small and would hence only induce small shifts in Figure 5. These values have also been shown to be fairly independent of concentration.[5]

Crowder	Partial specific volume (mL/g)	Reference
Ficoll 70	0.65	Christiansen, A., Wang, Q., Samiotakis, A., Cheung, M. S., Wittung-Stafshede, P. *Biochemistry* **2010**, *49*, 6519.
Ficoll 400	0.65	
Dextran 6	0.65	
Dextran 40	0.65	
BSA	0.733	Aldrich product specification sheet
Ovalbumin	0.750	Gagen, W.L. Biochemistry 1966, 5, 2553

Table S5: Hydrodynamic radii (σ) used in the scaling models.

Crowder	Hydrodynamic radius (nm)	Reference
Ficoll 70	5.1	GE Life Sciences product information sheet
Ficoll 400	10	
Dextran 6	1.8	Aldrich product information sheet, and Armstrong, J. K.; Wenby, R. B.; Meiselman, H. J.; Fisher, T. C. *Biophys. J.* **2004**, *87*, 4259.
Dextran 40	4.8	
BSA	3.5	Axelsson, I. *J. Chromatography A* **1978**, *152*, 21.
Ovalbumin	2.8	Bio-rad product information sheet
γ-Globulins	5.1	

Figures:

For control experiments on the crowding sensing and general properties of the GE probe we refer to ref. 9.

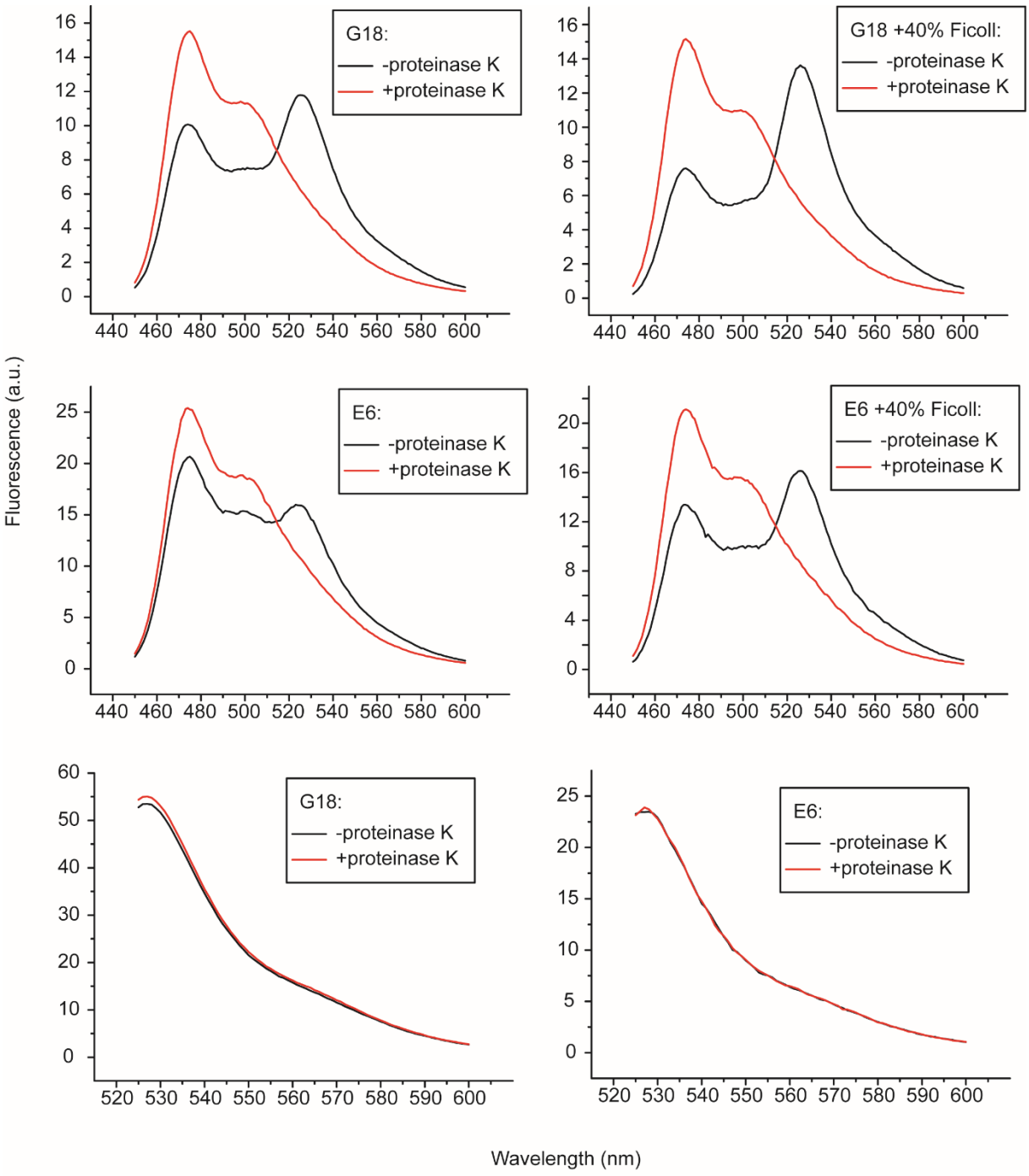

Figure S1. Fluorescence spectra of the G18 and E6 probes before and after proteinase K treatment, both with and without 40% w/w Ficoll 70. After treatment, FRET disappears leaving only the spectrum of mCerulean3. The increase in mCerulean3 fluorescence was used to determine the FRET efficiency using Eq. 1. The lower two graphs are the direct excitation of the mCitrine, as a control to confirm intact fluorophores after treatment. Furthermore, direct excitation of YFP after cleavage and comparison of the intensities with the CFP intensity after

cleavage shows that all the probes give the same YFP/CFP ratio of 3.2±0.4 (also in the presence of Ficoll), and hence the linker does not influence the maturation efficiency of YFP and/or CFP.

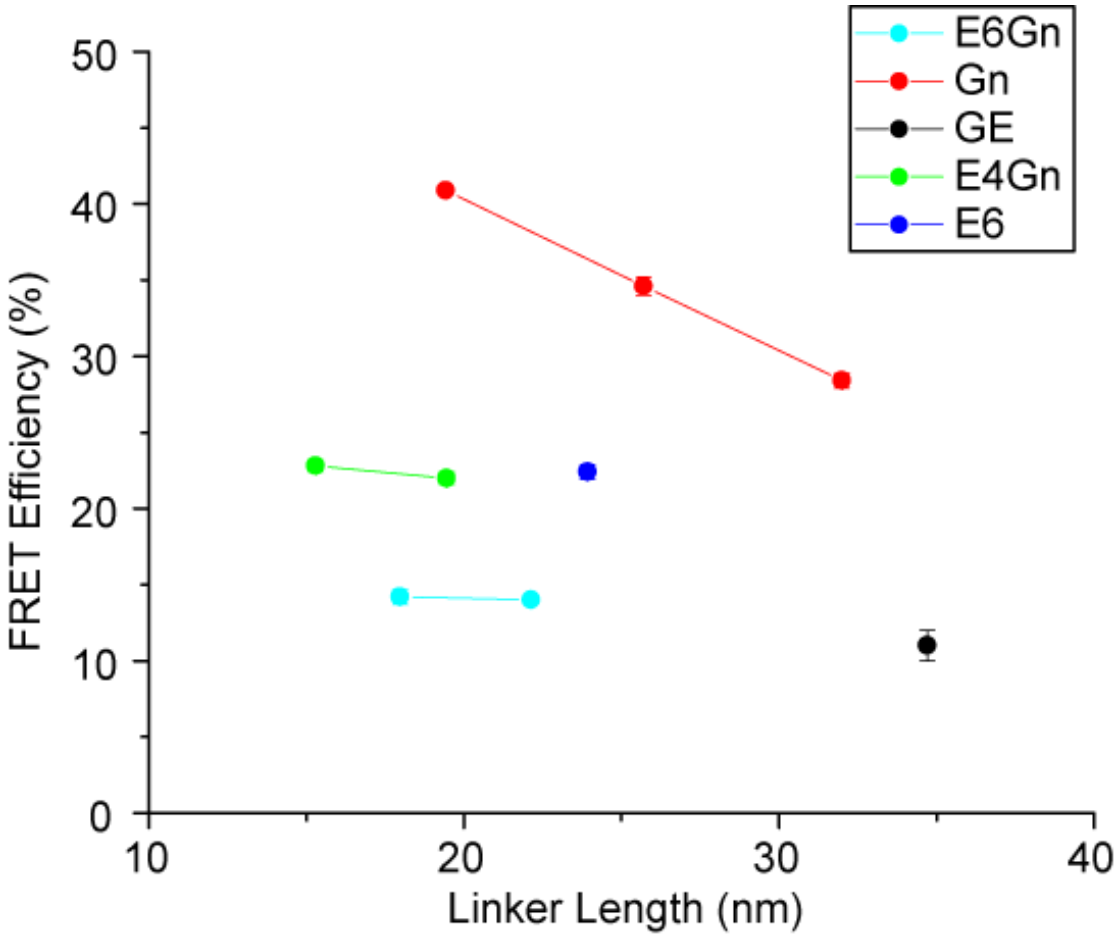

Figure S2. FRET efficiency as a function of linker length for the different families. It is clear that the FRET efficiency depends on the presence and length of α-helices in the linker. Data was taken from Table 1 and Table S3.

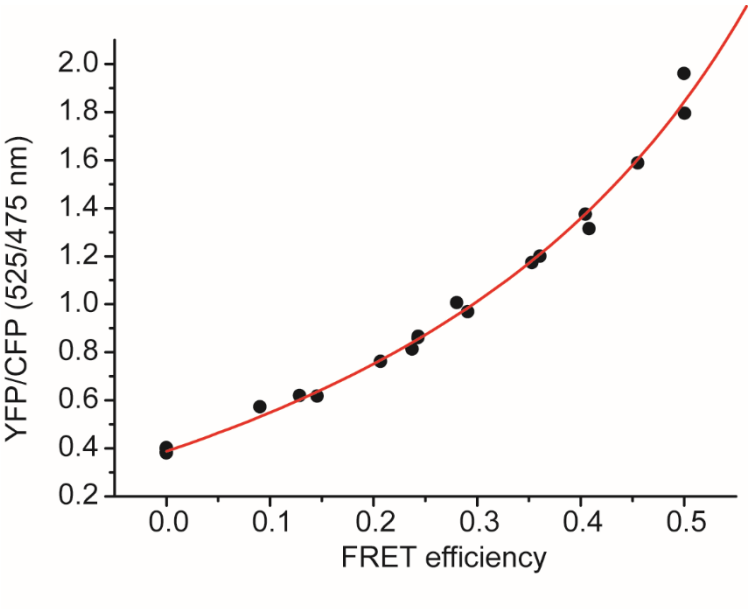

Figure S3. Empirical relation between YFP/CFP ratios and FRET efficiencies. Data correspond to the GE, E6G6, E6G2, E4G6, E4G2, E6, G24, G18, and G12 probes, at 0 and 40 % w/w Ficoll 70 in 10 mM NaPi, 100 mM NaCl, 2 mg/mL BSA, pH 7.4. All data points are evaluated using cleaving with proteinase K (see methods, as in Figure S1 and Table 1). The 0.0 FRET efficiency data points (which includes data from all 9 probes, but which are virtually indistinguishable) correspond to the YFP/CFP ratios of the cleaved probes. (Solid line) Fit to data, resulting in the relation $y = -1.455/(x - 1) - 1.068$.

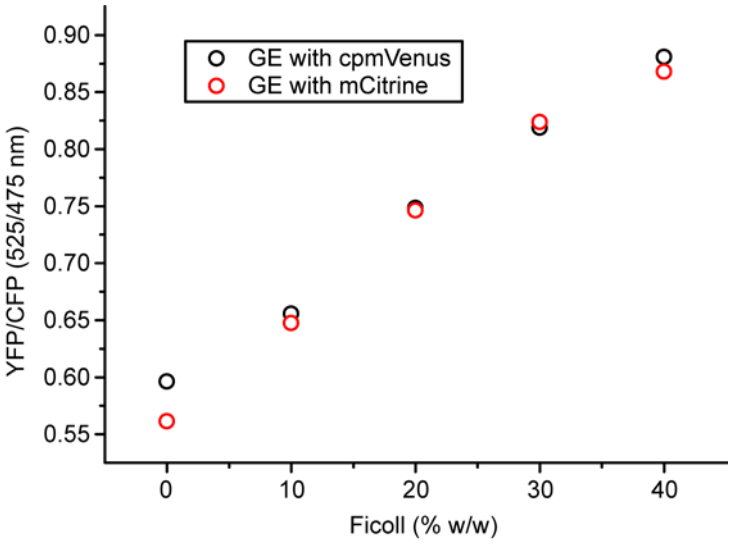

Figure S4. Comparison of the effect of Ficoll on the GE probes with different YFPs, i.e. mCitrine or circular permuted mVenus (cpmVenus). In cpmVenus the native N- and C-terminus are fused with a GGSGG linker, and a new N- and C-terminus is introduced in a loop on the other side of the barrel (the amino acid sequences can be found below). This results in the fluorescent protein to be upside down. In principle placing a fluorescent protein upside down would give the same FRET efficiency because the dipole of the fluorophore is unchanged (the fluorophore is perpendicular to the axis of the barrel, hence the direction of the dipole will not change). If changes are seen with circular permuted proteins it is due to fluorophore dimerization (GFPs also crystallize as antiparallel dimers), or other interactions that prevent free tumbling of the protein. The proteins in our case contain the A206K mutation to ensure monomeric fluorescent proteins. The YFPs do not have a similar brightness, with the cpmVenus excited at 515 nm being 30% more bright than mCitrine. The brightness levels do not change by addition of Ficoll. The increase in brightness gives a marginal increase in YFP/CFP ratio, which is small due to the cross talk of CFP emission into the YFP channel.[9] It can be seen that the results for both probes are nearly superimposable, indicating that the fluorescent proteins move freely in all cases.

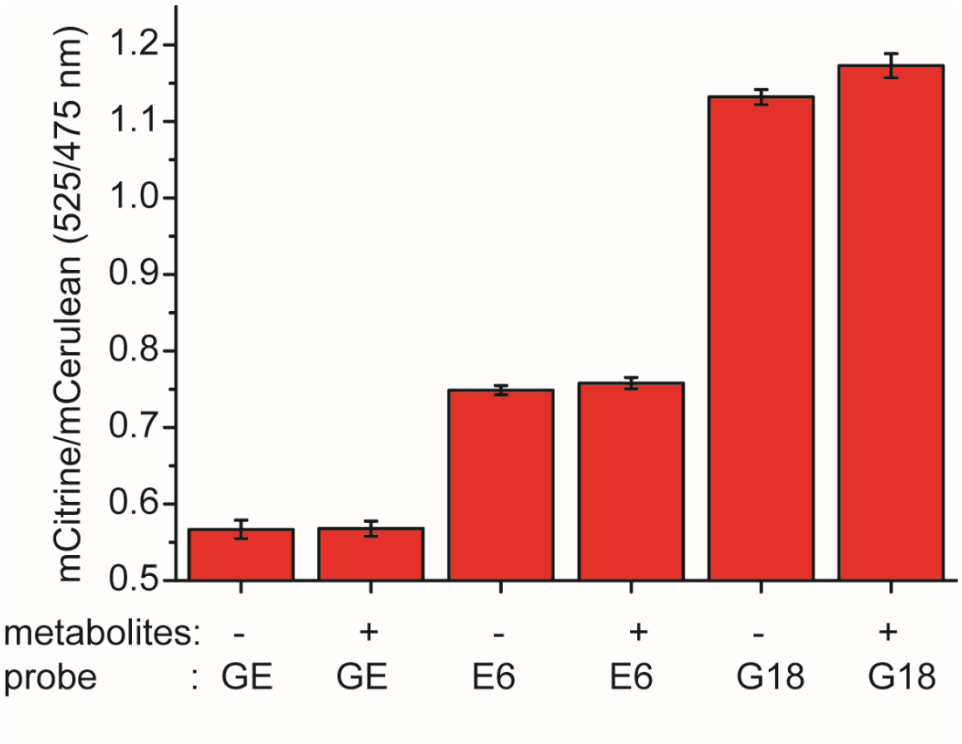

Figure S5. Effects of a mixture of the four most common metabolites in *E. coli* on the mCitrine/mCerulean3 emission ratio of the probes. We used a freshly prepared mixture of 100 mM glutamate, 20 mM glutathione, 15 mM fructose bisphosphate, and 10 mM ATP, in 10 mM NaP_i, and the pH was set to pH 7.4 with NaOH after dissolution of all solutes. Error bars represent the standard deviation of three independent experiments.

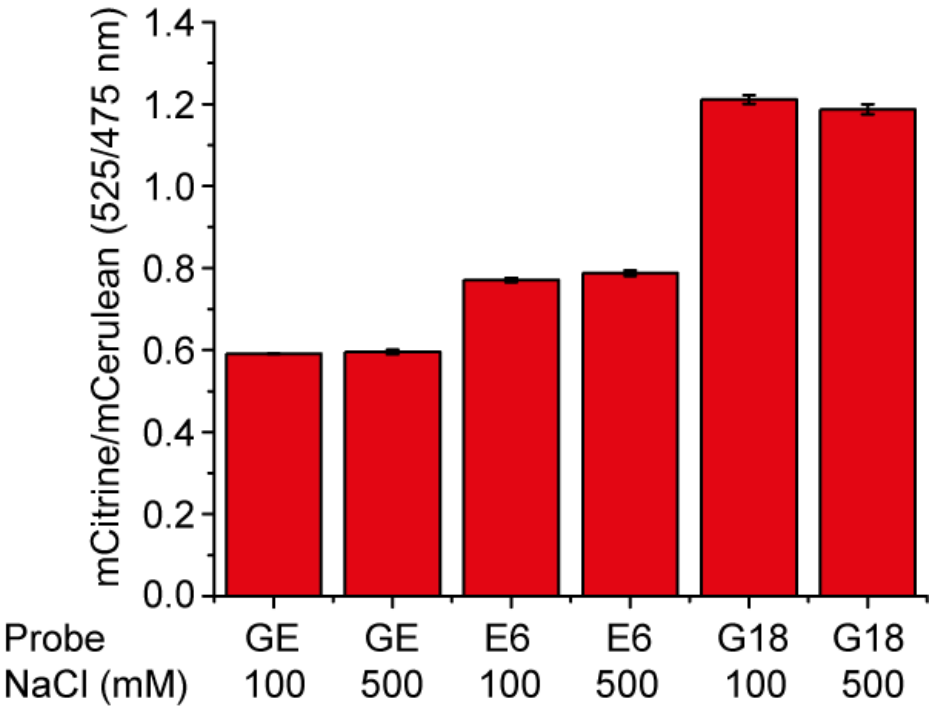

Figure S6. Addition of up to 500 mM NaCl did not influence the mCitrine/mCerulean3 ratios of purified GE, E6, and G18 probes; measurements were done in 10 mM NaPi, 2 mg/mL BSA, pH 7.4.

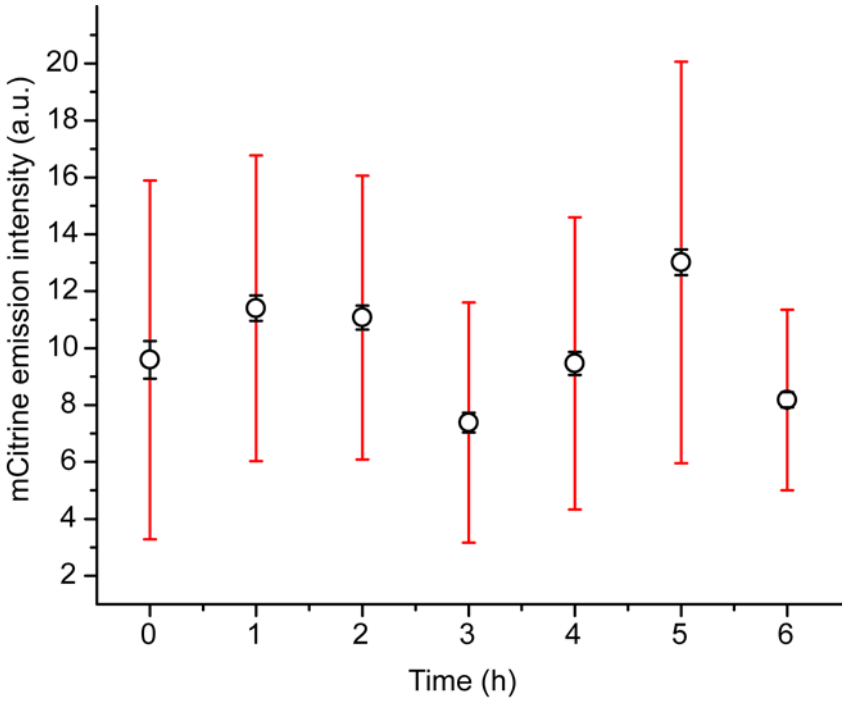

Figure S7. Expression of the G18 probe over time determined from mCitrine emission in fluorescence confocal microscopy (excitation 405 nm, emission 505-750 nm). The cells are grown at 30 ºC in MOPS minimal medium. The OD was kept between 0.1 – 0.2 by dilution. The averages of over >100 cells are given, the red error bars are the standard deviations denoting the spread of intensities found within a single population of cells; the black error bars are the standard error of the mean. The data shows that the expression of the probes is balanced with the growth rate of the cells, maintaining similar concentrations over time.

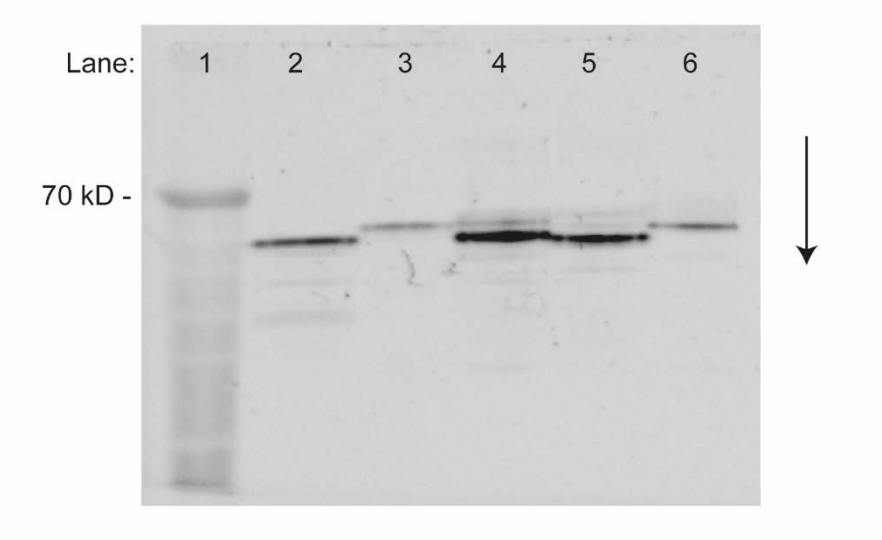

Figure S8. In-gel fluorescence SDS-PAGE analysis of the expression quality of the probes. Cells were grown in MOPS minimal medium at 30 ºC and harvested at an OD_{600} of 0.1-0.2. Cells were spun down and the cell pellet resuspended in 10 mM NaP_i, 100 mM NaCl, pH 7.4, supplemented with PMSF. The cells were lysed by tissue lyser and the lysate was directly loaded on the SDS-PAGE (10% polyacrylamide) gel. The gel was imaged by fluorescence using excitation at 460 nm, filter 515 nm. Integration of the fluorescent bands by ImageJ shows >95% purity. Lane 1: Marker, lane 2: G18, lane 3: G12, lane 4: E6, lane 5: E6G2, lane 6: GE.

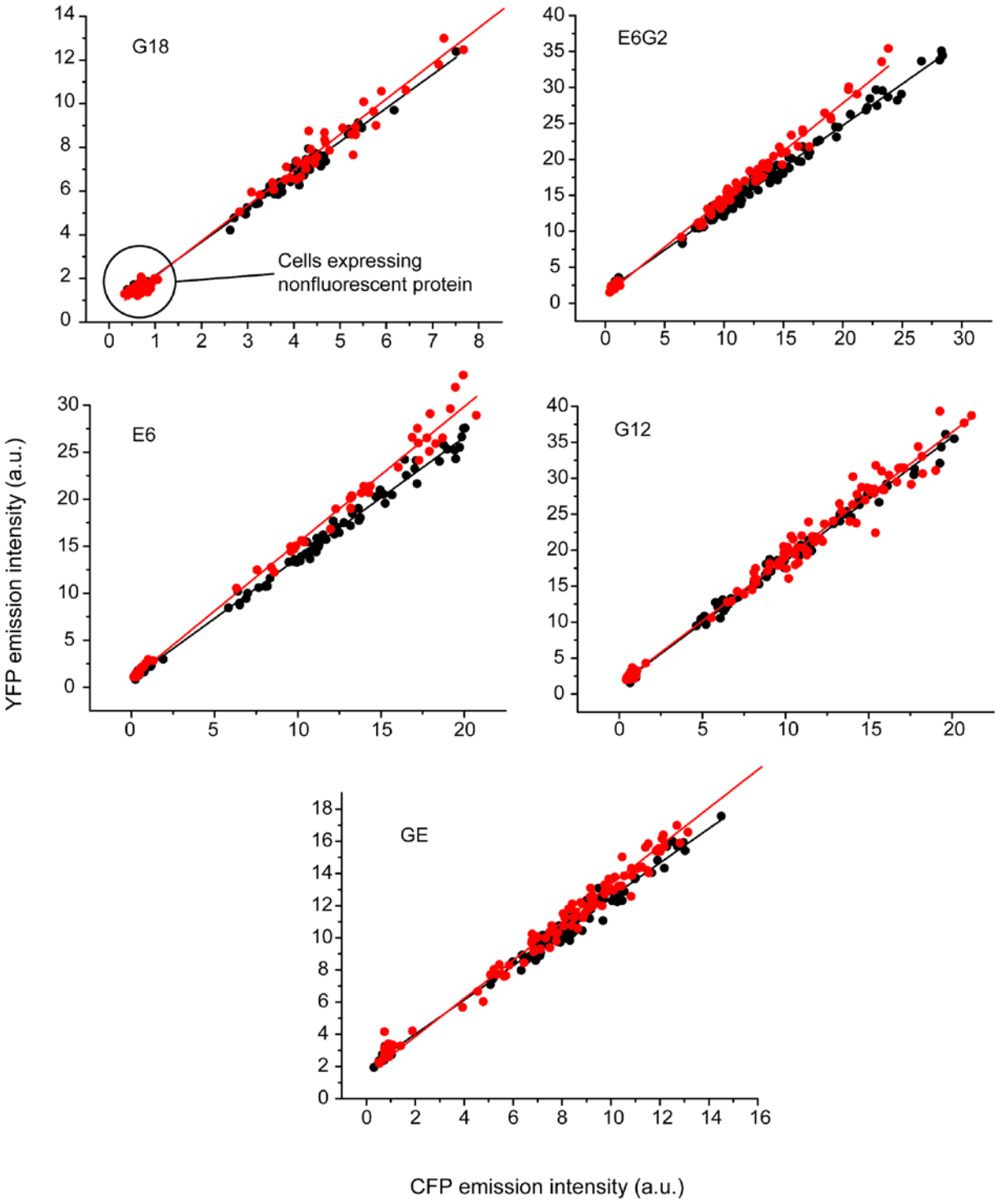

Figure S9. Representative examples of *in cell* YFP emission intensity *versus* CFP emission intensity acquired by confocal microscopy to determine YFP/CFP ratios. The low fluorescence population is *E. coli* cells expressing a non-fluorescent protein under the same conditions added to the full population. Each data point represents a single cell, and the results from all cells were fit to a line. The black data corresponds to cells before osmotic upshift; the red data corresponds to cells after 500 mM NaCl upshift. The R^2 values are in all cases > 0.985. The linear fit shows that the FRET ratio is independent on the emission intensity in the measured range.

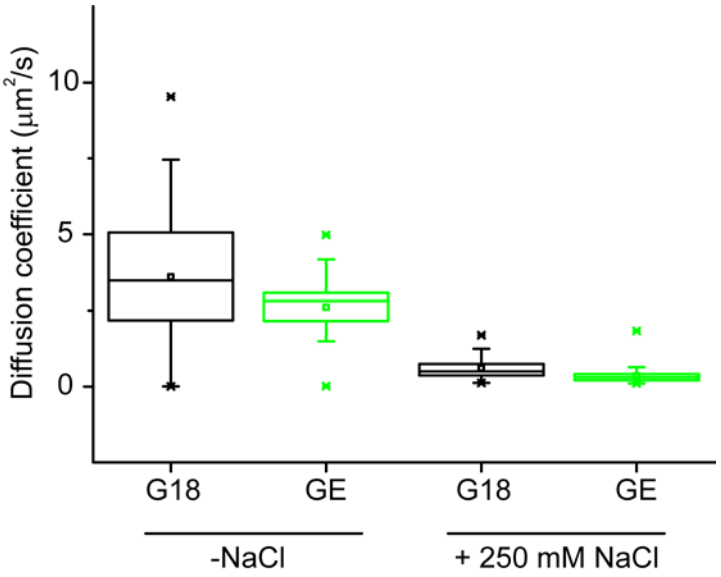

Figure S10. Diffusion coefficients of the G18 and GE probes in *E. coli* BL21, growing in MOPS minimal medium, with and without added 250 mM NaCl, as determined by FRAP. The diffusion coefficient at 500 mM NaCl was too slow to be observed. Under similar conditions in *E. coli*, GFP diffuses with a diffusion coefficient of 6-12 $\mu m^2/s$.[8] The difference in lateral diffusion constant can be explained by the larger size (and shape) of the sensors as compared to GFP.[10]

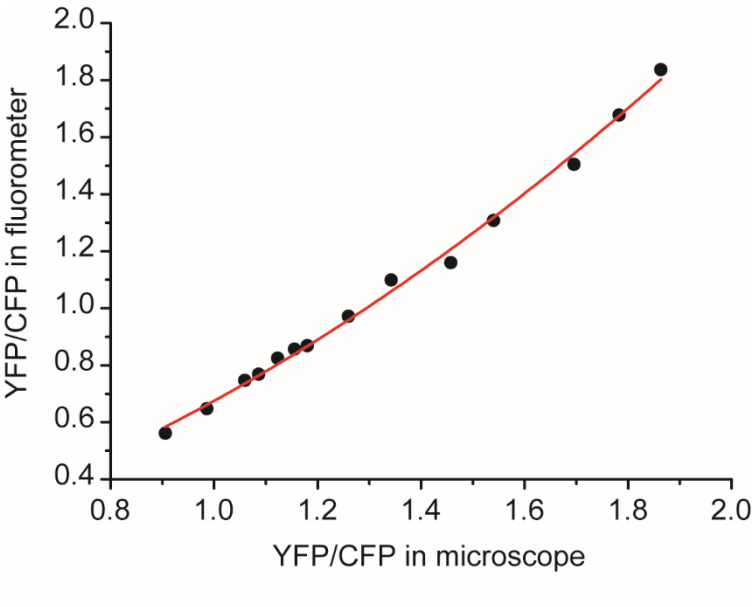

Figure S11. Empirical relation between YFP/CFP ratios determined by fluororescence spectrophotometer and by fluorescence microscope. The experimental data is the G18, E6, and GE probes, with 0, 10, 20, 30, and 40% w/w Ficoll 70, in 10 mM NaP_i, 100 mM NaCl, 2 mg/mL BSA, pH 7.4. These ratios span the whole range of ratios that we measure in the experiments. The data fits a polynomial $y = 0.02733 + 0.29485x + 0.35293x^2$, with $R^2 = 0.995$. The fit depends on multiple parameters that may not scale linearly: 1) The detection sensitivities of the two instruments over the whole spectrum range are not the same. 2) For the fluorometer it is the maximum intensity (at 475 and 525), while for the microscope it is a large wavelength range intensity that is measured (450-505 and 505-700). 3) Different contributions of emission bleed-through (CFP into YFP, and YFP into CFP) because the emission is determined differently on the two instruments.

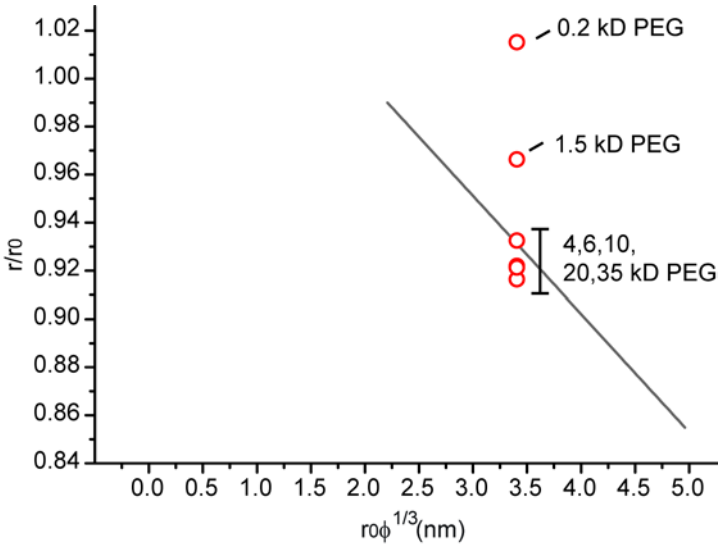

Figure S12. Dependence of compression on PEG size: For weights >4 kD, the compression no longer dependence on the size of the PEG and converges to the "calibration line" of Figure 5C. Data is at 10% w/w PEG with the GE probe.

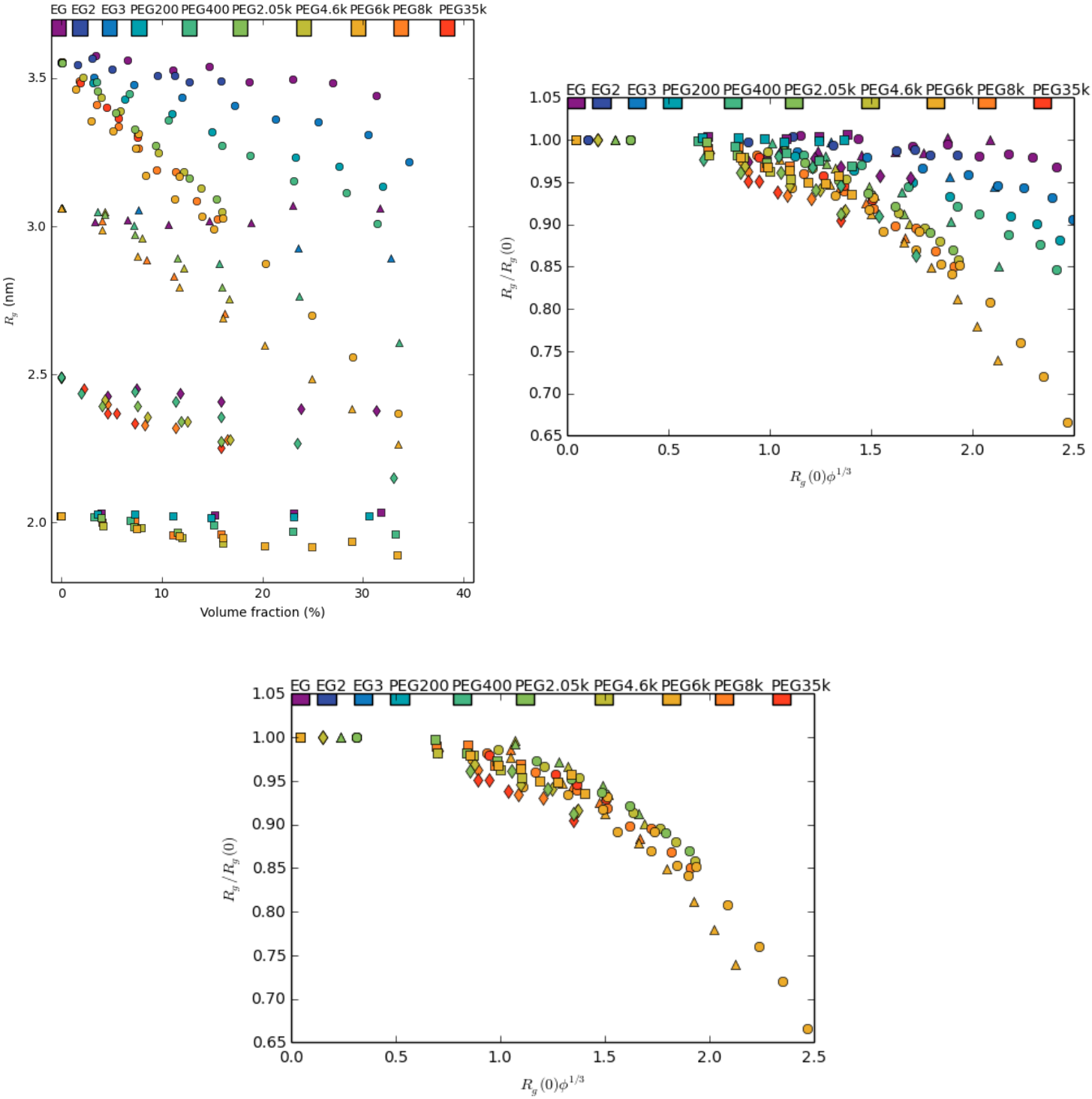

Figure S13. Reanalysis of measurement data of Schuler and coworkers[6] using the scaling *ansatz* from Kang *et al.*[7] (*A*) Radii of gyration (R_g) of four intrinsic disordered proteins ProTα-C (circles), ProTα-N (triangles), ACTR (diamonds), and IN (squares) in the presence of PEGs of varying molecular weight *versus* the volume fraction of PEG (φ). Data directly reproduced from ref. 19. (*B*) Data plotted as the relative compression $R_g(\varphi)/R_g(0)$ *versus* $R_g(0)\varphi^{1/3}$, that is, according to the scaling *ansatz* as described in the main text. (*C*) Same as panel B, but with the PEGs <1.5 kD omitted showing how the data follows a master curve with striking similarity to the probes used in this work, depicted in Figure 5C.

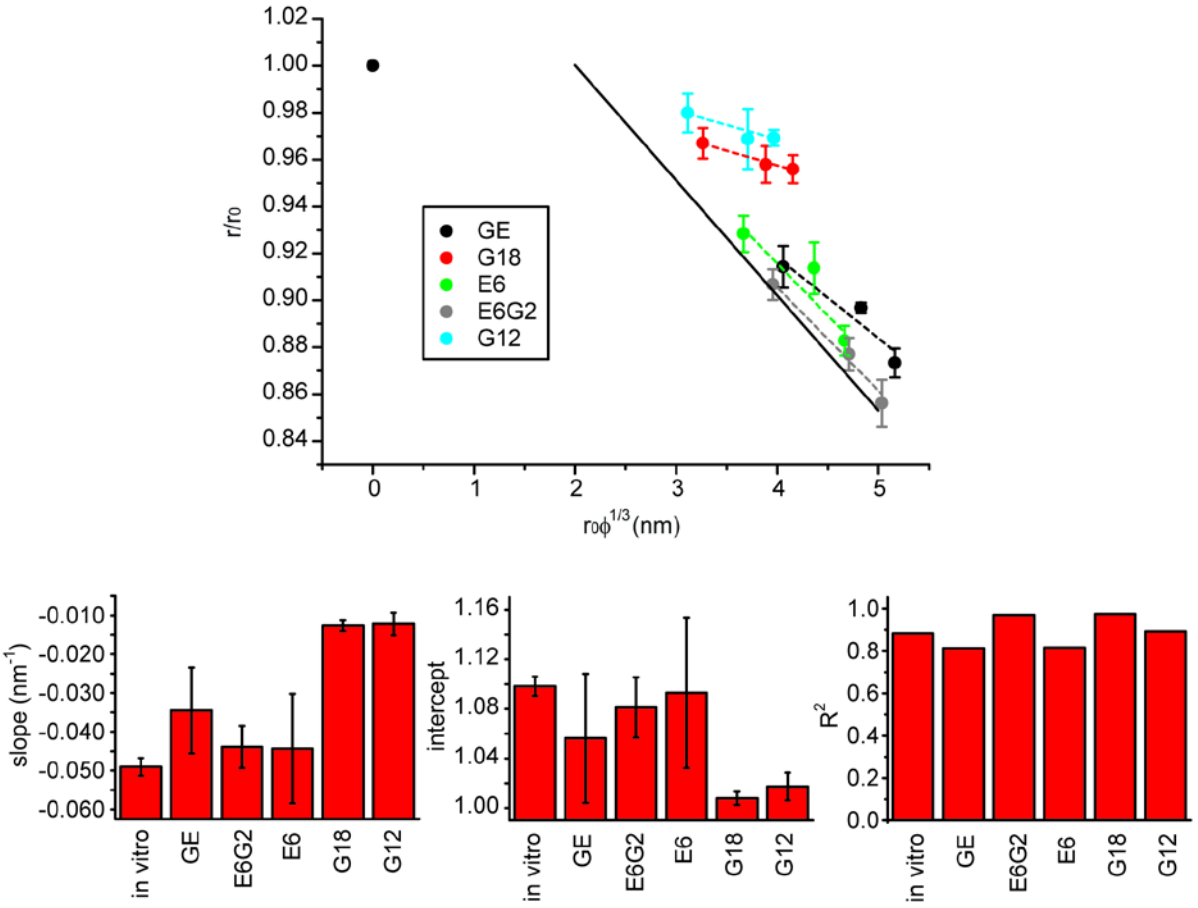

Figure S14. Comparison of the *in vitro* calibration with *in cell* compressions of the helix containing probes (E6, GE, and E6G2) and the probes that do not contain a helix (G18 and G12). The data is from Figure 5D and the individual probes fitted to a linear function. The bar graphs show the comparison of the slopes, intercepts and R^2 of the linear fits. Clearly, helix-lacking probes deviate inside the cells. The errors in the bar graphs are the standard errors from the fits.

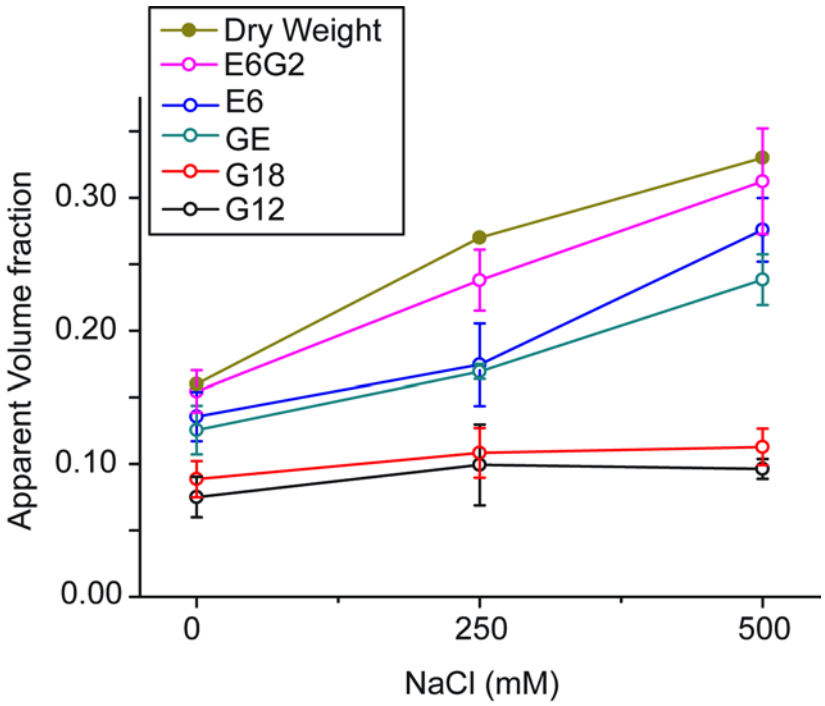

Figure S15. Apparent volume fraction sensed by the probes calculated with the calibration line of Figure 5C, and comparison with volume fractions determined from literature[8] (φ = 0.16, 0.27, 0.33, for 0, 250, 500 mM added NaCl respectively).

Amino acid sequences of the probes

G12:
HHHHHHVSKGEELFTGVVPILVELDGDVNGHKFSVSGEGEGDATYGKLTLKFICTTG
KLPVPWPTLVTTLSWGVQCFARYPDHMKQHDFFKSAMPEGYVQERTIFFKDDGNYK
TRAEVKFEGDTLVNRIELKGIDFKEDGNILGHKLEYNAIHGNVYITADKQKNGIKANF
GLNCNIEDGSVQLADHYQQNTPIGDGPVLLPDNHYLSTQSKLSKDPNEKRDHMVLLE
FVTAAGITLGMDELYKGSGGSGGSGGSGGSGGSGGSGGSGGSGGSGGSGGSMVSKG
EELFTGVVPILVELDGDVNGHKFSVSGEGEGDATYGKLTLKFICTTGKLPVPWPTLVT
TFGYGLMCFARYPDHMKQHDFFKSAMPEGYVQERTIFFKDDGNYKTRAEVKFEGDT
LVNRIELKGIDFKEDGNILGHKLEYNYNSHNVYIMADKQKNGIKVNFKIRHNIEDGSV
QLADHYQQNTPIGDGPVLLPDNHYLSYQSALSKDPNEKRDHMVLLEFVTAAGITLG
MDELYK

G18:
HHHHHHVSKGEELFTGVVPILVELDGDVNGHKFSVSGEGEGDATYGKLTLKFICTTG
KLPVPWPTLVTTLSWGVQCFARYPDHMKQHDFFKSAMPEGYVQERTIFFKDDGNYK
TRAEVKFEGDTLVNRIELKGIDFKEDGNILGHKLEYNAIHGNVYITADKQKNGIKANF
GLNCNIEDGSVQLADHYQQNTPIGDGPVLLPDNHYLSTQSKLSKDPNEKRDHMVLLE
FVTAAGITLGMDELYKGSGGSGGSGGSGGSGGSGGSGGSGGSGGSGGSGGSGGSGG
SGGSGGSGGSGGSMVSKGEELFTGVVPILVELDGDVNGHKFSVSGEGEGDATYGKLT
LKFICTTGKLPVPWPTLVTTFGYGLMCFARYPDHMKQHDFFKSAMPEGYVQERTIFF
KDDGNYKTRAEVKFEGDTLVNRIELKGIDFKEDGNILGHKLEYNYNSHNVYIMADK
QKNGIKVNFKIRHNIEDGSVQLADHYQQNTPIGDGPVLLPDNHYLSYQSALSKDPNE
KRDHMVLLEFVTAAGITLGMDELYK

G24:
HHHHHHVSKGEELFTGVVPILVELDGDVNGHKFSVSGEGEGDATYGKLTLKFICTTG
KLPVPWPTLVTTLSWGVQCFARYPDHMKQHDFFKSAMPEGYVQERTIFFKDDGNYK
TRAEVKFEGDTLVNRIELKGIDFKEDGNILGHKLEYNAIHGNVYITADKQKNGIKANF
GLNCNIEDGSVQLADHYQQNTPIGDGPVLLPDNHYLSTQSKLSKDPNEKRDHMVLLE
FVTAAGITLGMDELYKGSGGSGGSGGSGGSGGSGGSGGSGGSGGSGGSGGSGGSGG
SGGSGGSGGSGGSGGSGGSGGSGGSGGSGGSMVSKGEELFTGVVPILVELDGDVNG
HKFSVSGEGEGDATYGKLTLKFICTTGKLPVPWPTLVTTFGYGLMCFARYPDHMKQ
HDFFKSAMPEGYVQERTIFFKDDGNYKTRAEVKFEGDTLVNRIELKGIDFKEDGNILG
HKLEYNYNSHNVYIMADKQKNGIKVNFKIRHNIEDGSVQLADHYQQNTPIGDGPVLL
PDNHYLSYQSALSKDPNEKRDHMVLLEFVTAAGITLGMDELYK

E4G2:
HHHHHHVSKGEELFTGVVPILVELDGDVNGHKFSVSGEGEGDATYGKLTLKFICTTG
KLPVPWPTLVTTLSWGVQCFARYPDHMKQHDFFKSAMPEGYVQERTIFFKDDGNYK
TRAEVKFEGDTLVNRIELKGIDFKEDGNILGHKLEYNAIHGNVYITADKQKNGIKANF

GLNCNIEDGSVQLADHYQQNTPIGDGPVLLPDNHYLSTQSKLSKDPNEKRDHMVLLE
FVTAAGITLGMDELYKAEAAAKEAAAKEAAAKEAAAKAGSGGSGAEAAAKEAAAK
EAAAKEAAAKAMVSKGEELFTGVVPILVELDGDVNGHKFSVSGEGEGDATYGKLTL
KFICTTGKLPVPWPTLVTTFGYGLMCFARYPDHMKQHDFFKSAMPEGYVQERTIFFK
DDGNYKTRAEVKFEGDTLVNRIELKGIDFKEDGNILGHKLEYNYNSHNVYIMADKQ
KNGIKVNFKIRHNIEDGSVQLADHYQQNTPIGDGPVLLPDNHYLSYQSALSKDPNEK
RDHMVLLEFVTAAGITLGMDELYK

E4G6:
HHHHHHVSKGEELFTGVVPILVELDGDVNGHKFSVSGEGEGDATYGKLTLKFICTTG
KLPVPWPTLVTTLSWGVQCFARYPDHMKQHDFFKSAMPEGYVQERTIFFKDDGNYK
TRAEVKFEGDTLVNRIELKGIDFKEDGNILGHKLEYNAIHGNVYITADKQKNGIKANF
GLNCNIEDGSVQLADHYQQNTPIGDGPVLLPDNHYLSTQSKLSKDPNEKRDHMVLLE
FVTAAGITLGMDELYKAEAAAKEAAAKEAAAKEAAAKAGSGGSGGSGGSGGSGGS
GAEAAAKEAAAKEAAAKEAAAKAMVSKGEELFTGVVPILVELDGDVNGHKFSVSG
EGEGDATYGKLTLKFICTTGKLPVPWPTLVTTFGYGLMCFARYPDHMKQHDFFKSA
MPEGYVQERTIFFKDDGNYKTRAEVKFEGDTLVNRIELKGIDFKEDGNILGHKLEYN
YNSHNVYIMADKQKNGIKVNFKIRHNIEDGSVQLADHYQQNTPIGDGPVLLPDNHYL
SYQSALSKDPNEKRDHMVLLEFVTAAGITLGMDELYK

E6G2:
HHHHHHVSKGEELFTGVVPILVELDGDVNGHKFSVSGEGEGDATYGKLTLKFICTTG
KLPVPWPTLVTTLSWGVQCFARYPDHMKQHDFFKSAMPEGYVQERTIFFKDDGNYK
TRAEVKFEGDTLVNRIELKGIDFKEDGNILGHKLEYNAIHGNVYITADKQKNGIKANF
GLNCNIEDGSVQLADHYQQNTPIGDGPVLLPDNHYLSTQSKLSKDPNEKRDHMVLLE
FVTAAGITLGMDELYKAEAAAKEAAAKEAAAKEAAAKEAAAKEAAAKAGSGGSGA
EAAAKEAAAKEAAAKEAAAKEAAAKEAAAKAGGSKGEELFTGVVPILVELDGDVN
GHKFSVSGEGEGDATYGKLTLKFICTTGKLPVPWPTLVTTFGYGLMCFARYPDHMK
QHDFFKSAMPEGYVQERTIFFKDDGNYKTRAEVKFEGDTLVNRIELKGIDFKEDGNIL
GHKLEYNYNSHNVYIMADKQKNGIKVNFKIRHNIEDGSVQLADHYQQNTPIGDGPV
LLPDNHYLSYQSALSKDPNEKRDHMVLLEFVTAAGITLGMDELYK

E6G6:
HHHHHHVSKGEELFTGVVPILVELDGDVNGHKFSVSGEGEGDATYGKLTLKFICTTG
KLPVPWPTLVTTLSWGVQCFARYPDHMKQHDFFKSAMPEGYVQERTIFFKDDGNYK
TRAEVKFEGDTLVNRIELKGIDFKEDGNILGHKLEYNAIHGNVYITADKQKNGIKANF
GLNCNIEDGSVQLADHYQQNTPIGDGPVLLPDNHYLSTQSKLSKDPNEKRDHMVLLE
FVTAAGITLGMDELYKAEAAAKEAAAKEAAAKEAAAKEAAAKEAAAKAGSGGSGG
SGGSGGSGGSGAEAAAKEAAAKEAAAKEAAAKEAAAKEAAAKAMVSKGEELFTGV
VPILVELDGDVNGHKFSVSGEGEGDATYGKLTLKFICTTGKLPVPWPTLVTTFGYGL
MCFARYPDHMKQHDFFKSAMPEGYVQERTIFFKDDGNYKTRAEVKFEGDTLVNRIE
LKGIDFKEDGNILGHKLEYNYNSHNVYIMADKQKNGIKVNFKIRHNIEDGSVQLADH
YQQNTPIGDGPVLLPDNHYLSYQSALSKDPNEKRDHMVLLEFVTAAGITLGMDELYK

E6:
HHHHHHVSKGEELFTGVVPILVELDGDVNGHKFSVSGEGEGDATYGKLTLKFICTTG
KLPVPWPTLVTTLSWGVQCFARYPDHMKQHDFFKSAMPEGYVQERTIFFKDDGNYK
TRAEVKFEGDTLVNRIELKGIDFKEDGNILGHKLEYNAIHGNVYITADKQKNGIKANF
GLNCNIEDGSVQLADHYQQNTPIGDGPVLLPDNHYLSTQSKLSKDPNEKRDHMVLLE
FVTAAGITLGMDELYKGSGGSGGSGGSGGSGGSGAEAAAKEAAAKEAAAKEAAAK
EAAAKEAAAKAGSGGSGGSGGSGGSGGSMVSKGEELFTGVVPILVELDGDVNGHKF
SVSGEGEGDATYGKLTLKFICTTGKLPVPWPTLVTTFGYGLMCFARYPDHMKQHDFF
KSAMPEGYVQERTIFFKDDGNYKTRAEVKFEGDTLVNRIELKGIDFKEDGNILGHKLE
YNYNSHNVYIMADKQKNGIKVNFKIRHNIEDGSVQLADHYQQNTPIGDGPVLLPDNH
YLSYQSALSKDPNEKRDHMVLLEFVTAAGITLGMDELYK

GE:
HHHHHHVSKGEELFTGVVPILVELDGDVNGHKFSVSGEGEGDATYGKLTLKFICTTG
KLPVPWPTLVTTLSWGVQCFARYPDHMKQHDFFKSAMPEGYVQERTIFFKDDGNYK
TRAEVKFEGDTLVNRIELKGIDFKEDGNILGHKLEYNAIHGNVYITADKQKNGIKANF
GLNCNIEDGSVQLADHYQQNTPIGDGPVLLPDNHYLSTQSKLSKDPNEKRDHMVLLE
FVTAAGITLGMDELYKGSGGSGGSGGSGGSGGSGAEAAAKEAAAKEAAAKEAAAK
EAAAKEAAAKAGSGGSGGSGGSGGSGGSGAEAAAKEAAAKEAAAKEAAAKEAAA
KEAAAKAGSGGSGGSGGSGGSGGSMVSKGEELFTGVVPILVELDGDVNGHKFSVSG
EGEGDATYGKLTLKFICTTGKLPVPWPTLVTTFGYGLMCFARYPDHMKQHDFFKSA
MPEGYVQERTIFFKDDGNYKTRAEVKFEGDTLVNRIELKGIDFKEDGNILGHKLEYN
YNSHNVYIMADKQKNGIKVNFKIRHNIEDGSVQLADHYQQNTPIGDGPVLLPDNHYL
SYQSALSKDPNEKRDHMVLLEFVTAAGITLGMDELYK

GE probe with mCitrine and mCerulean3 swapped:
HHHHHHVSKGEELFTGVVPILVELDGDVNGHKFSVSGEGEGDATYGKLTLKFICTTG
KLPVPWPTLVTTLSWGVQCFARYPDHMKQHDFFKSAMPEGYVQERTIFFKDDGNYK
TRAEVKFEGDTLVNRIELKGIDFKEDGNILGHKLEYNAIHGNVYITADKQKNGIKANF
GLNCNIEDGSVQLADHYQQNTPIGDGPVLLPDNHYLSTQSKLSKDPNEKRDHMVLLE
FVTAAGITLGMDELYKGSGGSGGSGGSGGSGGSGAEAAAKEAAAKEAAAKEAAAK
EAAAKEAAAKAGSGGSGGSGGSGGSGGSGAEAAAKEAAAKEAAAKEAAAKEAAA
KEAAAKAGSGGSGGSGGSGGSGGSMVSKGEELFTGVVPILVELDGDVNGHKFSVSG
EGEGDATYGKLTLKFICTTGKLPVPWPTLVTTFGYGLMCFARYPDHMKQHDFFKSA
MPEGYVQERTIFFKDDGNYKTRAEVKFEGDTLVNRIELKGIDFKEDGNILGHKLEYN
YNSHNVYIMADKQKNGIKVNFKIRHNIEDGSVQLADHYQQNTPIGDGPVLLPDNHYL
SYQSALSKDPNEKRDHMVLLEFVTAAGITLGMDELYK

GE probe with mCitrine replaced for circular permuted mVenus:
HHHHHHVSKGEELFTGVVPILVELDGDVNGHKFSVSGEGEGDATYGKLTLKFICTTG
KLPVPWPTLVTTLSWGVQCFARYPDHMKQHDFFKSAMPEGYVQERTIFFKDDGNYK

TRAEVKFEGDTLVNRIELKGIDFKEDGNILGHKLEYNAIHGNVYITADKQKNGIKANF
GLNCNIEDGSVQLADHYQQNTPIGDGPVLLPDNHYLSTQSKLSKDPNEKRDHMVLLE
FVTAAGITLGMDELYKGSGGSGGSGGSGGSGGSGAEAAAKEAAAKEAAAKEAAAK
EAAAKEAAAKAGSGGSGGSGGSGGSGGSGAEAAAKEAAAKEAAAKEAAAKEAAA
KEAAAKAGSGGSGGSGGSGGSGGSMDGGVQLADHYQQNTPIGDGPVLLPDNHYLS
YQSKLSKDPNEKRDHMVLLEFVTAAGITLGMDELYKGGSGGMVSKGEELFTGVVPI
LVELDGDVNGHKFSVSGEGEGDATYGKLTLKLICTTGKLPVPWPTLVTTLGYGLQCF
ARYPDHMKQHDFFKSAMPEGYVQERTIFFKDDGNYKTRAEVKFEGDTLVNRIELKGI
DFKEDGNILGHKLEYNYNSHNVYITADKQKNGIKANFKIRHNIE

SUPPORTING REFERENCES

(1) J.T. Mika, P.E. Schavemaker, V. Krasnikov, B. Poolman, Impact of osmotic stress on protein diffusion in Lactococcus lactis, Mol. Microbiol. 94 (2014) 857-870.
(2) J.T. Mika, V. Krasnikov, G. van den Bogaart, F. de Haan, B. Poolman, Evaluation of pulsed-FRAP and conventional-FRAP for determination of protein mobility in prokaryotic cells, Plos One 6 (2011) e25664.
(3) Doi, M (1996) In Introduction to Polymer Physics, Clarendon Press, Oxford, UK.
(4) de Gennes, PG (1979) In Scaling Concepts in Polymer Physics, Cornell University Press, Ithaca, N.Y.
(5) A. Christiansen, Q. Wang, A. Samiotakis, M.S. Cheung, P. Wittung-Stafshede, Factors defining effects of macromolecular crowding on protein stability: an in vitro/in silico case study using Cytochrome C, Biochemistry 49 (2010) 6519-6530.
(6) A. Soranno, I. König, M.B. Borgia, H. Hofmann, F. Zosel, D. Nettels, B. Schuler, Single-molecule spectroscopy reveals polymer effects of disordered proteins in crowded environments, Proc. Natl. Acad. Sci. U. S. A. 111 (2014) 4874-4879.
(7) H. Kang, P.A. Pincus, C. Hyeon, D. Thirumalai, Effects of macromolecular crowding on the collapse of biopolymers, Phys. Rev. Lett. 114 (2015) 068303
(8) M.C. Konopka, K.A. Sochacki, B.P. Bratton, I.A. Shkel, M.T. Record, J.C. Weisshaar, Cytoplasmic protein mobility in osmotically stressed Escherichia coli, J. Bacteriol. 191 (2009) 231-237.
(9) A.J. Boersma, I.S. Zuhorn, B. Poolman, A sensor for quantification of macromolecular crowding in living cells, Nat. Methods 12 (2015) 227-229.
(10) J.T. Mika, B. Poolman, Macromolecule diffusion and confinement in prokaryotic cells, Curr. Opin. Biotechnol. 22 (2011) 117-126.